

# UV-Visible Measurements of Metallic Nanoparticles for Sensing Applications

## Introduction

Nanomaterials have been extensively researched for use in a myriad of different applications, including catalysis, chemical/biochemical sensing, and drug delivery.<sup>1-3</sup> These materials can come in a variety of sizes and shapes as well as material type (organic, metallic, semiconducting, etc.). In particular, metallic nanoparticles are widely studied due in part to their unique localized surface plasmon resonance (LSPR). This resonance is produced in noble metal materials, like gold (Au) and silver (Ag), when light of a frequency resonant with that of the oscillation of conducting electrons impinges on the sample.<sup>3-5</sup> This results in sharp absorption and scattering features, often in the visible range of the electromagnetic spectrum, allowing for the use of UV-Visible absorption techniques for characterization.

The resonant wavelength for plasmonic nanomaterials, like Ag or Au nanoparticles, is dependent on a number of properties such as size, shape, or dielectric function. For example, the dielectric function of the material influences the position and peak width of the LSPR peak in the UV-Visible spectrum.<sup>3</sup> For aqueous dispersions of Ag nanoparticles, this typically results in yellow solution with a maximum LSPR peak close to 400 nm while Au nanoparticles suspended in the same medium will appear red ( $\lambda_{\text{max}} = 525 \text{ nm}$ ).<sup>6</sup> Additionally, changes in the location of the LSPR peak can be observed by tuning the size or the shape (e.g., sphere vs rod) of the nanomaterial.<sup>3,7</sup>

In addition to these properties, the absorption spectra of plasmonic materials also depend on the sample environment, such as pH and passivating ligand.<sup>3</sup> For example, the position of the LSPR band is dependent on the dielectric function of the surrounding medium, and by extension its refractive index.<sup>3,7,8</sup> This sensitivity to the local environment can lead to subtle shifts in the position of the nanomaterial's LSPR peak in the UV-Visible region. As such, UV-Visible analysis can be used to monitor these changes in the presence of different analytes, acting as a form of chemical sensor.<sup>3,5</sup>

In addition to sensing the changes in the refractive index of the local medium, other methods of detection involve aggregation of the dispersed nanomaterials.<sup>4,9-15</sup> As the aggregates form, a new LSPR peak related to the population of aggregated particles grows in at longer (redshifted) wavelengths and broadens, while typically a concomitant loss of the original LSPR peak is observed.<sup>4,9,12</sup> In this way, a change in the apparent color of the solution can be observed, leading to a colorimetric indication of the presence of the analyte which induced the aggregation. Depending on the sample conditions, these aggregates may be small enough to not scatter light or large enough to produce a broad scattering artifact across the UV-Visible region.

As such, it can be highly important to characterize the changes observed in the UV-Visible region as the sample environment changes.

Regardless of the sensing method used, many of these applications inherently require the use of UV-Visible techniques to characterize the nanoparticles studied and/or monitor the behavior of these substances in the presence of different analytes. To demonstrate these analyses, both Au and Ag nanoparticles were measured using the Thermo Scientific™ GENESYS™ 180 UV-Visible Spectrophotometer under different sample conditions. Through these experiments, the sensitivity of the measured absorption spectrum based on the sample environment was outlined, demonstrating the need for UV-Visible analysis when characterizing plasmonic nanomaterials. Additionally, the ability to measure traditional absorption spectra of small nanoparticles without the need for additional instrument accessories was shown.

## Experimental

### Sample Preparation

Ag and Au nanoparticle solutions were purchased and used as received. The Ag nanoparticles were dispersed in 2 mM sodium citrate while the Au nanoparticles were dispersed in 0.1 mg/mL sodium citrate. The diameter of the nanoparticles for both samples was expected to be 20 nm according to the manufacturer's specifications. A 20 mM stock solution of sodium citrate was prepared and further diluted to produce two separate sodium citrate buffer solutions with concentrations of 2 mM and 0.1 mg/mL sodium citrate. These solutions were used for further dilutions of the stock Ag and Au solutions to keep the citrate concentration consistent.

Control samples were made by diluting 667  $\mu\text{L}$  of the stock nanoparticle solution with enough of the respective sodium citrate solution to achieve a volume of 2 mL total. Two Ag nanoparticle samples were made containing nanoparticles in 10% and 25% v/v ethanol (EtOH) in sodium citrate buffer. The same procedure was repeated using the Au nanoparticle solution as well. The amount of each component used to prepare these solutions is described in Table 1. For the salt-induced aggregation experiment, 667 mL of the stock Ag nanoparticles was diluted to 2 mL using 1X phosphate buffer saline solution (PBS). The solution was allowed to equilibrate for a few minutes prior to UV-Visible analysis.

**Table 1. Preparation of Ag and Au nanoparticles in the presence of varying amounts of ethanol.**

Sample	Amount of nanoparticle solution* ( $\mu\text{L}$ )	Amount of absolute ethanol ( $\mu\text{L}$ )	Amount of sodium citrate solution** (mL)
10% v/v EtOH in buffer	667	200	1.133
25% v/v EtOH in buffer		500	0.833

**\*The same sample preparation was carried out for both Ag and Au nanoparticle solutions.**

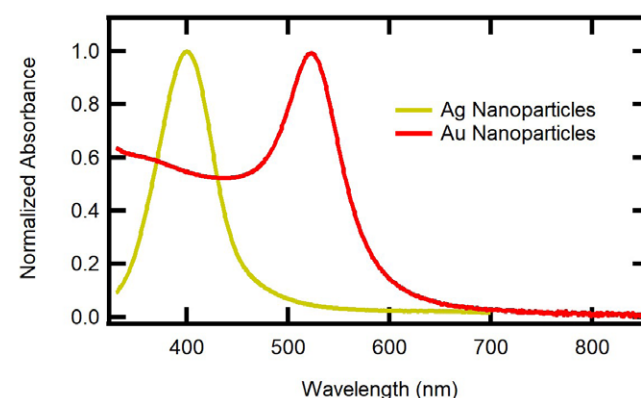
**\*\*The appropriate sodium citrate solution was used for dilution based on the citrate concentration in the stock solution (2 mM for Ag nanoparticles and 0.1 mg/mL for Au nanoparticles).**

### Instrumentation

For all samples prepared, UV-Visible spectra were collected using the Thermo Scientific GENESYS 180 Spectrophotometer. Measurements were collected using a 1.0 nm data interval and slow scan rates. All samples were held in a 1.0 cm polystyrene cuvette during data acquisition.

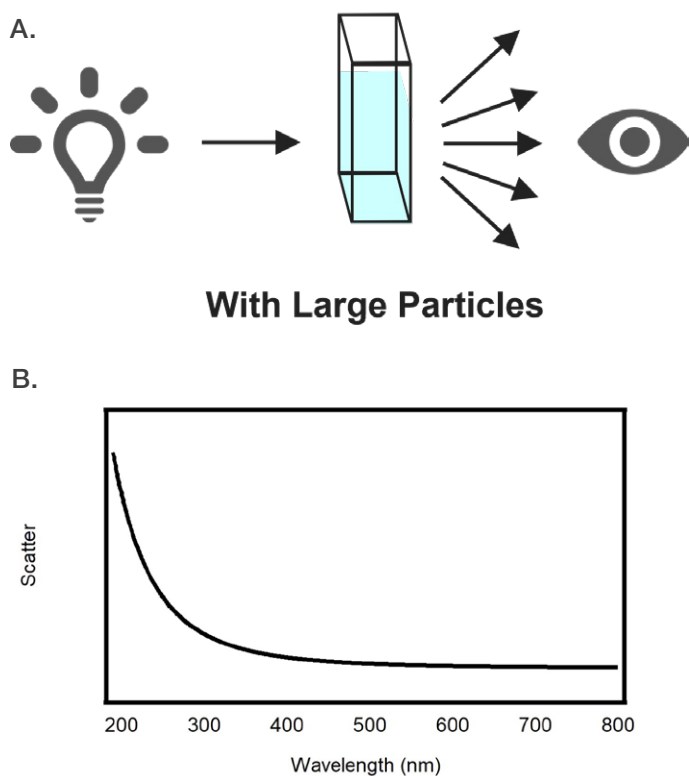
### Results/Discussion

Figure 1 includes the normalized absorption spectra of aqueous Ag and Au nanoparticle suspensions. The absorption maxima were observed at 400 nm and 523 nm for the Ag and Au solutions, respectively. These observations are similar to those reported in literature.<sup>6</sup> As particles are known to scatter light, often a broad, non-linear apparent absorption feature can be observed across the UV-Visible spectrum.



**Figure 1. Normalized UV-Visible spectra of (red) gold nanoparticles and (yellow) silver nanoparticles. Spectra were collected using a 1.0 cm quartz cuvette. Each spectrum was normalized using the respective absorption maximum.**

This feature arises from the light intensity loss as the scattered light is directed away from the instrument detector (Figure 2), which the instrument incorrectly attributes to absorption by the sample. The presence of a scattering artifact can often be an issue when interpreting spectra, as correction can be difficult. Typically, this is overcome by using an integrating sphere to collect diffuse reflectance or transmittance measurements of the material. As integrating spheres are capable of collecting scattered light, this artifact can be minimized, and a cleaner spectrum can be reported. Notably, little to no scattering artifact was observed in the samples included in Figure 1, suggesting nanoparticles of similar size (~20 nm) can be easily measured through standard transmission measurements, avoiding the need for accessories like integrating spheres.



**Figure 2. (a) Depiction of light transmission for a scattering solution. The eye icon refers to the instrument detector. (b) Example of a scattering artifact across the UV-Visible spectrum.**

As discussed earlier, changes in the local environment can influence the LSPR peak position for materials like Ag and Au nanoparticles due to the dependence of peak location on dielectric function. To demonstrate this behavior, nanoparticle samples dispersed in solutions of varying EtOH:aqueous buffer content were analyzed using UV-Visible absorption spectroscopy. For these samples, subtle changes can be observed in the LSPR band for both Ag and Au nanoparticles. As EtOH content increases to 10% and 20%, the absorbance increases for each type of nanoparticle.

A small redshift in the absorption maximum from 400 nm to 405 nm was observed for the Ag nanoparticle solutions (Figure 3a). However, the LSPR peak position for the Au nanoparticles did not shift (Figure 3b).

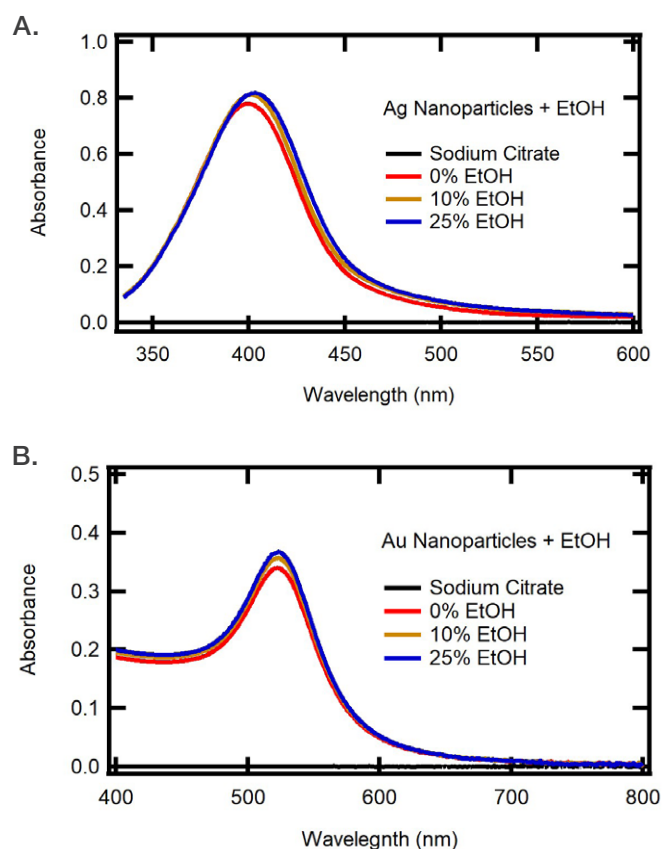


**Figure 3. Absorption spectra of (a) Ag and (b) Au nanoparticles in aqueous EtOH mixtures. All spectra were measured using a 1.0 cm polystyrene cuvette.**

The small degree of shifting in the Ag LSPR peak is in line with expectations based on the difference in refractive index of water and EtOH,<sup>3,8</sup> though larger shifts have been observed previously with different Ag nanomaterials.<sup>8</sup> The lack of change in the band maximum position for the Au nanoparticles may instead be a result of the lesser refractive index sensitivity expected for Au nanomaterials as compared to Ag. According to literature, the dielectric function for Ag nanoparticles allows for a higher sensitivity to the refractive index of the surrounding medium, while this sensitivity is lower for Au nanoparticles,<sup>3</sup> pointing toward a possible explanation for the discrepancies observed between the Ag and Au samples studied. The degree to which these peaks shift can also be dependent on the shape and size of the nanoparticles.<sup>7</sup> While the manufacturer indicates the nanoparticles are 20 nm in diameter for both solutions studied, further microscopy work would be needed to confirm the size distribution and shapes of the Ag and Au particles analyzed herein.

As described previously, some sensing-based applications involve the utilization of nanoparticles' aggregation as a colorimetric detection method.<sup>4</sup> In some cases, this aggregation is initiated through the introduction of salt to the solution which can screen the electrostatic interaction between the capping ligand and the metallic surface.<sup>4,13,14</sup> Depending on other sample parameters, these aggregates can shift the LSPR peak to longer wavelengths.<sup>9-14</sup> Alternatively, a broad feature spanning the full visible wavelength range can also be present if the aggregates are allowed to grow large enough to scatter light. To demonstrate this behavior, Figure 4 includes the absorption spectra for a set of Ag nanoparticles in the presence of PBS.

When PBS is introduced to the solution, a significant decrease in the absorption spectrum is observed, while a broad feature at longer wavelengths is also observed extending past the measured wavelength range. Similar observations as shown in Figure 4 have been reported previously.<sup>10,11</sup> The broad feature at longer wavelengths, where PBS does not absorb, suggests the nanoparticles have aggregated with the introduction of PBS, as expected based on literature.<sup>10,11</sup> This is further corroborated by the loss of the LSPR peak at 400 nm.

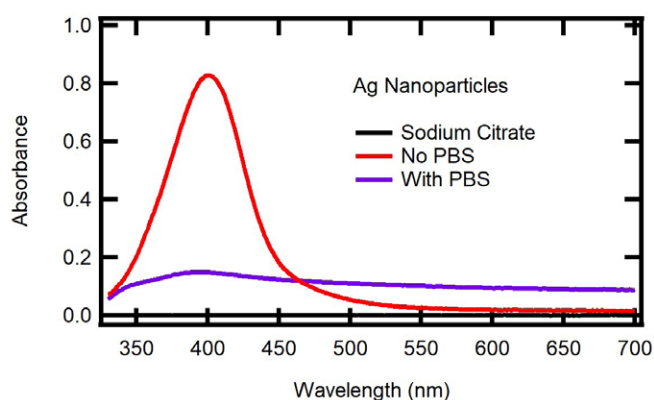


**Figure 4 - Absorption spectra of Ag nanoparticles with (purple) and without (red) PBS present. The black curve is the absorption spectrum of 2 mM sodium citrate.**

As the newly formed broad absorption feature extends out past the measurement range, this feature implies PBS not only initiated the aggregation of the particles, but that the particle agglomerates are large enough to scatter light. Based on literature,<sup>11,15</sup> the positively charged counter ions ( $\text{Na}^+$  and  $\text{K}^+$ ) in PBS are likely screening the charge of the passivating citrate ligands on the nanoparticle surface. By disrupting the electrostatic interaction between citrate and Ag, the nanoparticles are no longer stable and will agglomerate. As a clear scattering feature is present, this further implies the phosphate ions in solution are unable to passivate the surface of the nanoparticles and prevent formation of large aggregates, though further work would be needed for confirmation.

While the UV-Visible spectrum included in Figure 4 does include a broad scattering artifact, this does not inherently suggest this technique cannot be used to analyze this nanoparticle system. For quantification purposes, the presence of light scatter can skew the calculated concentration and should be corrected for, typically through the use of an integrating sphere as described previously. However, for studies which do not require quantification, the presence of a scattering artifact can be a useful signature for spectral interpretation. For the Ag nanoparticle spectra collected using the GENESYS 180 spectrophotometer, the scattering signal was used to indicate the buffer solution was initiating aggregation of the particles, as described earlier. These results outline the feasibility of transmission UV-Visible techniques without the use of an integrating sphere in the analysis of some materials.

## Conclusion

The results outlined herein exhibit the sensitivity of Ag and Au nanoparticles' UV-Visible spectra to the sample environment, in agreement with literature. This susceptibility to sample conditions makes UV-Visible analysis a highly useful tool when analyzing plasmonic nanoparticles, especially for sensing applications. Additionally, the ability to reliably analyze nanoparticles samples using the GENESYS 180 UV-Visible spectrophotometer is established, as the measurements obtained here agree with literature. Furthermore, the analysis of scattering substances for qualitative spectral interpretations is highlighted without the need to use a separate instrument accessory.

## References

1. Xie, C.; Niu, Z.; Kim, D.; Li, M.; Yang, P., Surface and Interface Control in Nanoparticle Catalysis, *Chem. Rev.*, 2020, 120, 1184 – 1249.
2. Blanco, E.; Shen, H.; Ferrari, M., Principles of Nanoparticle Design for Overcoming Biological Barriers to Drug Delivery, *Nat. Biotechnol.*, 2015, 22, 941 – 951.
3. Mayer, K. M.; Hafner, J. H., Localized Surface Plasmon Resonance Sensors, *Chem. Rev.*, 2011, 111, 3828 – 3857.
4. Vilela, D.; González, M. C.; Escarpa, A., Sensing Colorimetric Approaches Based on Gold and Silver Nanoparticles Aggregation: Chemical Creativity Behind the Assay. A Review., *Anal. Chim. Acta*, 2012, 751, 24 – 43.
5. Svedendahl, M.; Chen, S.; Käll, M., An Introduction to Plasmonic Refractive Index Sensing, In *Nanoplasmonic Sensors*, New York, NY, Springer, 2012, 1 – 26. DOI: 10.1007/978-1-4614-3933-2\_1.
6. Wulandari, P.; Fukada, N.; Kimura, Y.; Niwano, M.; Tamada, K. Characterization of Citrate on Gold and Silver Nanoparticles, *J. Colloid Interface Sci*, 2015, 438, 244 – 248.
7. Chen, H.; Kou, X.; Yang, Z.; Ni, W.; Wang, J., Shape- and Size-Dependent Refractive Index Sensitivity of Gold Nanoparticles, *Langmuir*, 2008, 24, 5233 – 5237.
8. Chen, H.; Ming, T.; Zhao, L.; Wang, F.; Sun, L.-D.; Wang, J.; Yan C.-H., Plasmon-Molecule Interactions, *Nano Today*, 2010, 5, 494 – 505.
9. Kanjanawarut, R.; Su, X., Colorimetric Detection of DNA Using Unmodified Metallic Nanoparticles and Peptide Nucleic Acid Probes, *Anal. Chem.*, 2009, 81, 6122 – 6129.
10. Trisaranakul, W.; Chompoosor, A.; Maneeprakorn, W.; Nacapricha, D.; Choengchan, N.; Teerasong, S., A Simple and Rapid Method Based on Anti-Aggregation of Silver Nanoparticles for Detection of Poly(diallyldimethylammonium chloride) in Tap Water, *Anal. Sci.*, 2016, 32, 769 – 773.
11. Afshinnia, K.; Baalousha, M., Effect of Phosphate Buffer on Aggregation Kinetics of Citrate-Coated Silver Nanoparticles Induced by Monovalent and Divalent Electrolytes, *Sci. Total Environ.*, 2017, 581, 268 – 276.
12. Abbasian, S.; Moshaii, A.; Nikkiah, M.; Farkhari, N., Adsorption of DNA on Colloidal AG Nanoparticles: Effects of Nanoparticle Surface Charge, Base Content and Length of DNA, *Colloids Surf. B Biointerfaces*, 2014, 116, 439 – 445.
13. Gearheart, L.A.; Ploehn, H.J.; Murphy, C.J., Oligonucleotide Adsorption to Gold Nanoparticles: A Surface-Enhanced Raman Spectroscopy Study of Intrinsically Bent DNA, *J. Phys. Chem. B*, 2001, 105, 12609 – 12615.
14. Li, H.; Rothberg, L., Colorimetric Detection of DNA Sequences Based on Electrostatic Interactions with Unmodified Gold Nanoparticles, *PNAS*, 2004, 101, 14036 – 14039.
15. Wang, Y.; Quinsaat, J.E.Q.; Ono, T.; Maeki, M.; Tokeshi, M.; Isono, T.; Tajima, K.; Satoh, T.; Sato, S.-I.; Miura, Y.; Yamamoto, T., Enhanced Dispersion Stability of Gold Nanoparticles by the Physisorption of Cyclic Poly(ethylene glycol), *Nat. Commun.*, 2020, 11, 6089.

 Learn more at [thermofisher.com/genesys](https://thermofisher.com/genesys)

thermo scientific

For research use only. Not for use in diagnostic procedures. For current certifications, visit [thermofisher.com/certifications](https://thermofisher.com/certifications)

© 2024 Thermo Fisher Scientific Inc. All rights reserved. All trademarks are the property of Thermo Fisher Scientific and its subsidiaries unless otherwise specified. **MCS-AN1047-EN 5/24**